Maximizing light olefins and aromatics as high value base chemicals via single step catalytic conversion of plastic waste

Andreas Eschenbacher[a], *Robin John Varghese*[a], *Mehrdad SeifaliAbbas-Abadi*[a], *Kevin M. Van Geem*[a,*]

[a] Laboratory for Chemical Technology (LCT), Department of Materials, Textiles and Chemical Engineering, Faculty of Engineering & Architecture, Ghent University, Technologiepark 125, 9052 Zwijnaarde, Belgium

*Correspondence: Kevin.VanGeem@UGent.be; Tel.: +32 9 264 55 97

KEYWORDS. FCC; chemical recycling; plastics; upgrading; olefins; polyolefins; HZSM-5;

ABSTRACT

Chemical recycling of plastic waste via thermochemical processes is essential to move to a carbo-circular economy, reducing our dependence of fossil resources . However, recovering monomers from polyolefins in one or multiple steps is challenging due to their chemical inertness. In the present work, a tandem micro-pyrolyzer coupled to comprehensive two-dimensional gas chromatography and FID/ToF-MS detectors was utilized to study the performance of industrial formulations of steam-treated FCC catalysts and HZSM-5 additives for the in-line catalytic upgrading of polyolefin pyrolysis products towards light olefins and aromatics in two steps. When upgrading pyrolysis vapors from LDPE over the steam-treated catalysts at 600 °C, CH_4 yields did not exceed 0.5 wt% due to their low acidity. The FCC catalyst formulations obtained higher yields of C_5-C_{11} aliphatics (up to 42 wt%) and were more active in converting C_{12}+ products than the HZSM-5-containing additives. The highest C_2-C_4 olefin selectivity of 53 wt% was obtained using a bare steam-treated HZSM-5 additive. With this catalyst, at higher catalyst loading and temperature (700 °C), the light olefin yield reached 69 wt% (19% ethylene, 22% propylene, 10% 1,3-butadiene, and 18% other C_4 olefins). Importantly, similar yields of light olefins with even higher propylene yields of 31 wt% were obtained when processing real post-consumer mixed polyolefin waste. An adjusted loading of unsteamed catalyst (to obtain a similar level of initial conversion of C_{12}+ products) showed higher coking propensity and deactivated more rapidly than its steam-treated version. The research results show great potential for the pyrolysis of mixed polyolefin waste followed by the direct in-line upgrading of the pyrolysis vapors to produce high value base chemicals such as C_2-C_4 olefins, aromatics, and naphtha-range aliphatics at high selectivity while limiting formation of coke, CH_4, and H_2.

1 INTRODUCTION

Fossil-derived polyolefins account for about half of the world's plastics production and are commonly used in the packaging industry with a short product life-time [1]. Due to the unique properties of polyolefin

waste, the conventional methods of mechanical recycling lead to downcycling, i.e., to products with lower quality. Other waste disposal approaches such as landfilling and incineration come with several drawbacks [2]. Today, microplastics have penetrated the depths of the oceans, endangering many of micro and macro-organisms [3]. As a result of these detrimental impacts on the environment and in a strive for more circular economies, the interest for chemical recycling of plastic waste via thermochemical processes such as pyrolysis is on the rise [4–9]. Pyrolysis processes operate in the absence of oxygen and allow to convert a variety of polymers to gases, liquid/wax, and residue [10]. The product distribution depends on the type of feed [11,12], temperature [13], heating rate [14], catalyst type [15–18], carrier gas [19] and reactor type [20,21]. Using appropriate catalysts which increase the selectivity to high-value products can be an important step towards the industrialization of pyrolysis processes [22–24].

For several decades, FCC catalysts are commercially used to crack heavy hydrocarbon fractions such as gas oil and residue towards lighter hydrocarbons, preferably LPG and naphtha [25,26]. The typical catalyst formulation contains a microporous zeolite Y (FAU topology), mesoporous alumina and silica matrix active in pre-cracking larger molecules, and binders and fillers to provide physical strength and integrity [27]. Using FCC-type catalyst formulations for the processing of polyolefins has the potential to avoid scale-up issues [7], and it appears that these catalysts have high efficiency for the production of petroleum liquids from plastics [28,29]. FCC catalyst that has been in commercial operation is referred to as equilibrium catalyst, or E-Cat. E-Cat has a much lower activity compared to a fresh FCC catalyst due to poisoning of active sites by metal contaminants in the feed and the hydrothermal dealumination of the zeolite component during oxidative regeneration.

In recent years, the catalytic production of light olefins has become more important due to high demand and their high value as base chemicals. In FCC, strategies to increase the yield of light olefins include operating at higher severity, e.g., at increased reactor temperature and catalyst/feed ratio, and/or to add

HZSM-5 to the FCC formulation or physically add an olefin-enhancing HZSM-5 containing additive to the reactor [30]. The ZSM-5 component can be modified, e.g., by varying its Si/Al ratio, incorporation of mesopores, and metal addition to favor light olefin production during the catalytic cracking of hydrocarbons [31–33]. The hydrothermal stability of HZSM-5 can be improved by the addition of phosphorus [24,25,34–41] since the added phosphorus improves the stability of framework aluminum species against dealumination [30,37,42,43]. Advantageously, the P modification also improves the selectivity towards light olefins [34]. For catalytic pyrolysis of polyolefins, generally, higher yields of gaseous products and higher selectivities to light olefins were reported using fresh HZSM-5 compared to an equilibrium FCC catalysts [44,45], albeit this can hardly be regarded as a fair comparison without hydrothermally dealuminating also the HZSM-5 under similar FCC conditions.

Table 1 summarizes literature studies that used FCC-type catalysts for direct contact (=*in-situ*) catalytic fast pyrolysis (CFP) of polyolefins in the temperature range of 400-500 °C. Increasing the temperature from 450 to 515 °C increased the yield of C_2-C_4 olefins from 20 to 27 wt% for PE catalytic pyrolysis [46]. It is noteworthy that using an E-Cat compared to a fresh FCC catalyst lead to much lower coke yields due to the reduced acidity of the E-cat caused by the steam dealumination [27,47]. The rate and extent of deactivation of the catalyst by coking needs to be considered for industrial implementation [48,49]. The catalyst coke is often polyaromatic and/or high molecular weight polyaliphatic, which deactivates the catalysts by attaching to and covering active sites, eventually blocking pores, making other sites inaccessible [50,51]. Another study worth pointing out is the one by Olazar et al. [52], since these researchers used fresh, mildly steamed (5h at 760 °C) and severely steamed (8h at 816 °C) FCC catalysts for the catalytic pyrolysis of HDPE [52]. While the fresh FCC catalyst favored C_1-C_4 products, with increasing steaming severity the production of gasoline and eventually diesel-range hydrocarbons was

favored [52]. These results are not surprising since with increased steaming severity the acidity, closely linked to activity, and therefore the conversion decreased.

These prior investigations summarized in Table 1 used virgin-type plastics without inorganic contamination for degrading polyolefins in direct contact with FCC catalysts. For real-life postconsumer mixed polyolefin feed, some contamination with inorganics/metals is unavoidable. Consequently, the *in-situ* CFP has the shortcoming that the inorganics—in particular alkalines—in the feed would physically block and chemically poison acid sites [53,54]. In addition, the recovery of olefins in prior studies using FCC catalysts was fairly low, with C_2-C_4 olefin recoveries below 40 wt%. This is mainly attributed to the process parameters chosen in these works, particularly the moderate catalyst temperature.

Based on the insufficiency of existing research to study FCC catalysts under conditions suitable for production of high light olefin yields, in the present work, pyrolysis was first carried out in a thermal pyrolysis reactor, and the vapors were swept with a carrier gas over the catalyst placed in a second reactor. This two-stage strategy configuration of pyrolysis-catalytic cracking is referred to as ex-situ contact mode [55,56] and has been studied using different reactor types [57–61]. Advantageously, the pyrolysis and catalytic reactor temperature can be controlled independently, and even more importantly, it will mitigate the poisoning of acid sites by alkaline inorganics present in the real postconsumer waste, as was observed when processing ash-containing biomass [48,54,62]. The upgrading in the vapor phase also protects the catalyst from direct contact with asphaltenes/heavy waxes and the deposition of metal/char fines physically blocking pores. This configuration has a good potential for scale-up [18] but has been investigated to a minimal extent for FCC catalysts and FCC additives to the best of our knowledge. Only Onwudili et al. [18] investigated the *ex-situ* upgrading of polyolefin vapors from a mix of HDPE, LDPE, PP, PS, and PET at 500 °C over a E-Cat at 600 °C, reporting a fairly low yield of 21 wt% C_2-C_4 olefins.

Therefore, the primary goal of the present work was to investigate if a higher recovery of light olefins can be achieved by using steamed FCC catalysts and HZSM-5 additives as catalysts and operating at high catalyst/feed ratios and high catalyst temperatures of 600 and 700 °C. Steaming the catalysts under high severity prior to catalytic testing was done to limit the formation of coke, and, to facilitate scale-up considerations since the low activity remaining in an E-Cat or a catalyst steamed under high-severity can be regarded stable for the reaction conditions of polyolefins vapor upgrading. Therefore, the yields reported in this work will provide a more valid estimate for the yields that could be obtained in long-term operation with equilibrated catalysts compared to testing fresh catalysts. To summarize the objectives of the present work:

1) Testing of different steam-treated industrial FCC-type catalysts, HZSM-5 additives, and a commercial operated E-Cat containing HZSM-5 additive for the in-line (=ex-situ) upgrading the pyrolysis vapors derived from virgin PE and quantitatively comparing the product yields amongst the different catalysts.
2) Relating the product selectivities and yields to the catalyst properties and feed properties.
3) Investigating the effect of catalyst/feed ratio and catalyst temperature. To distinguish thermal from catalytic cracking, tests were also performed replacing the catalyst with highly inert low surface area α-Al_2O_3.
4) Using real (=contaminated) mixed polyolefin (MPO) feed to investigate the effect of catalyst deactivation by coke using the catalyst with the highest selectivity towards light olefins.

Table 1. Summary of studies investigating FCC-based catalysts with direct feed-catalyst contact (*in-situ* CFP)

Ref	Feed	Pyrolysis and catalyst T [°C]	Reactor	contact time	Catalyst/ Feed ratio	Catalyst	H_2 [wt%]	CH_4 [wt%]	C_2-C_4 Olefins [wt%]	Ethylene [wt%]	Propylene [wt%]	C_4 Olefins [wt%]	Aromatics [wt%]	C_{5-11} (excl. aromatics) [wt%]	C_{12}+ [wt%]	coke [wt%]
[46]	LDPE	515	fluid bed	medium (10 s)	1.7	E-Cat	0.1	2.1	26.8	1.5	12.4	12.9	8.9	24.6	5.5	9.2
[47]	HDPE	450	fluid bed	medium	6.0	fresh FCC	0.002		21.8	1.8	11	9	2.8			13.3
	HDPE	450	fluid bed	medium	6.0	E-Cat	0.001		31.51	0.61	9.8	21.1	0			1.3
[63]	LDPE dissolved in Toluene	500	riser simulator reactor	medium (12 s)	173	E-Cat	n.d.	n.d.	23.9	~2	8.4	14				10
[64]	40 wt% HDPE, 27 wt% LDPE, 33 wt% PP	450	fluid bed	medium	3.3	E-Cat	n.d.	<0.01	28.2	0.4	11.3	16.5	2.5	50.9	n.d.	2.9
[45]	38 wt% HDPE, 24 wt% LDPE, 30 wt% PP, 7% PS, 1% PVC	460	fluid bed	medium	3.3	E-Cat	n.d.	<0.01	24	0.2	8.2	15.6	2.7	50.6	n.d.	3
[65]	34 wt% HDPE, 30 wt% LDPE, 34 wt% PP	390	fluid bed	medium	5.0	E-Cat	n.d.	0.1	38.2	1.3	16.4	20.5	0.8	32.2	n.d.	3.6
[52]	HDPE	475	spouted bed	short	60[a]	steamed FCC	n.d.	0.23	6.5	0.9	2.4	3.2	5.8	23.1	54.4	<1
[66]	HDPE	500	spouted bed	short	30[a]	E-Cat + 50 wt% bentonine	n.d.		23	1	8	14	5	48	15	NA

[a]per minute

2 MATERIALS AND METHODS

2.1 Plastics Preparation and Characterization

Virgin LDPE Resin was obtained from ExxonMobil (LD150AC). Since the product was in pellet-form, it was pulverized using a cutting mill (FRITSCH). The obtained powder was sieved to obtain a fraction with particle size <300 µm which was used for the micropyrolysis tests to avoid mass and heat-transfer limitations. The post-consumer mixed polyolefinic waste (MPO) was prepared by cold-washing of sorted polyolefinic waste, with an approximate composition of 75 wt% PE, 16 wt% PP and 9 wt% rest, whereby the rest roughly consists of 2% PA, 1% PET, 1% PS, and 5% non-polymers. A CryoMill was used for pulverizing the MPO pellets to obtain particles <300 µm for the pyrolysis experiments.

The elemental CHNS/O composition of the milled MPO feedstock was analyzed nine times using a Thermo Scientific FLASH 2000 analyzer. 2-3 mg of sample was combusted in pure oxygen at 960 °C. Carbon is oxidized to CO_2, hydrogen to H_2O, sulfur to SO_2, and nitrogen is converted to nitrogen oxides which are then reduced over a copper catalyst to nitrogen by eliminating oxygen. The gas products are separated by gas chromatography coupled with a thermal conductivity detector (GC-TCD). The oxygen content was calculated by difference under consideration of any moisture (not the case for the polyolefin materials) and inorganics.

In addition, for the MPO feed the content of volatiles, fixed carbon, and inorganics (=ash) was determined by thermogravimetric analysis using a Netsch STA 449F3 instrument following similar procedures described for biomass feeds [67,68]. About 40 mg of sample was loaded in an alumina crucible and the temperature was first ramped to 105 °C at 10 °C/min in nitrogen atmosphere (100 ml/min) and held at that temperature for 40 min in order to remove any moisture. The content of volatiles was determined as the final weight loss when heated in N_2 from 105 to 900 °C at 10 °C/min and holding the final temperature at 900 °C for 20 min. To determine the fixed carbon

content, nitrogen was replaced by air and the temperature held at 900 °C for 30 min in order to combust the fixed carbon. The remaining mass after combustion of fixed carbon was considered ash.

To verify the ash content determined by TGA, according to ASTM D2584, D5630, and ISO 3451 methods, ~4 g of the ground virgin LDPE and MPO material were placed in two porcelain crucibles calcined in a muffle furnace at 600 °C under airflow. The remaining ash was gravimetrically determined.

2.2 Catalyst Preparation and Characterization

The E-Cat (FCC catalyst containing a physically mixed HZSM-5 additive) provided by TotalEnergies was subjected to calcination for 5 h at 550 °C to remove potential contaminants such as S-containing organics and combust any remaining carbonaceous deposits remaining from the commercial operation [64]. The content of HZSM-5 additive in the E-Cat was between 5% and 10%.

Two HZSM-5 additives and FCC formulations were provided by W.R. Grace & Co.-Conn (abbr. GRACE). These formulations had been steamed for 4 h at 815 °C by the manufacturer and were used directly as provided. GRACE Catalysts Technologies provided the analysis of catalyst properties such as ABD@1000, DI@1000, the total specific surface area (SA), the surface area of the matrix (SA-MX), the surface area of the zeolite (SA-ZE), and the elemental composition. In addition to the steamed catalysts, an unsteamed version of the high HZSM-5 content additive was provided. The Zeolite surface area was determined using nitrogen physisorption according to ASTM D4365. The acidity of the catalysts tested in this work (incl. the refinery E-Cat) was analyzed by NH_3-TPD using an AutoChem II instrument (Micromeritics). To summarize the procedure, ~300 mg of steamed catalysts material (~100 mg for unsteamed catalyst) were loaded in a U-shaped quartz tube supported on quartz wool. The loaded catalyst material was initially

pretreated by heating to 600 °C at 20 °C/min (final temperature hold time 30 min) in He flow to remove moisture. Then, the catalyst temperature was cooled to 100 °C under He flow, before admitting NH_3 (4% NH_3 in He) over the catalyst for 30 min. Weakly physisorbed NH_3 was flushed with pure He (60 mL/min) for 120 min, before starting the temperature-programmed NH_3-desorption (10 °C/min) while recording the desorbing NH_3 using a thermal conductivity detector (TCD). The response of the TCD detector was calibrated against different NH3 concentrations in the gas to allow for quantification of the desorbed NH3. Deconvolution of the desorption profile by Gaussian peak fitting was done using Origin 2018 software.

The coke deposition on the catalysts from single experiments amounted to less than 10 µg and therefore could not be accurately determined via the in-house available thermogravimetric and elemental analysis techniques. However, since for two catalysts the deactivation was investigated passing pyrolysis vapors from a large number of sample injections over the catalyst, significantly more coke had deposited for these tests . To quantify the carbon deposited on the catalyst, the catalyst was then transferred into tin capsules and subjected to elemental analysis as described in section 2.1.

2.3 Micro-Pyrolyzer

The pyrolysis tests were performed using a micro-pyrolyzer (Rx-3050 TR, Frontier Lab., Japan) coupled to both two-dimensional gas chromatography (GC) and a separate GC dedicated for analysis of light gases. 60 mL/min of He was used as the carrier gas in the micropyrolyzer, resulting in a catalyst contact time of ~0.08s, while at the point of reaction, the pressure of the GC inlet and inside the reactors was ~2.7 bara. The column flow was set to 2.1 mL/min. 400±20 µg of ground material was loaded with a high precision balance (±1 µg) into deactivated stainless steel sample cups (Eco-cup SF) and then dropped into the preheated pyrolysis furnace (550 °C). The carrier gas constantly purged volatiles into the second reactor, which contained a quartz tube with

the catalyst bed supported between quartz wool plugs. The products exiting the upgrading reactor entered the GC and were trapped inside the GC × GC oven by a cryo-trap (MJT-1035E) cooled with liquid nitrogen. The cryo-trap was held for 5 min and then switched off. During that time, the GC oven was held at -40 °C by cryogenic cooling. As soon as the cryo-trap was switched off, the column temperature increased to the oven temperature and trapped vapors were released in a refocused manner according to their boiling points. Downstream the cryo-trap, part of the column flow was branched to reach a customized multicolumn GC (Trace 1300) for light gas analysis. The oven temperature of the GC × GC was held at -40 °C for 8 minutes, followed by heating at 3 °C/min to 320 °C. A two stage cryogenic modulator (liquid CO_2) was positioned between the first and second dimension column (modulation time 5 s). The 1st dimension column was a non-polar RTX-1 PONA (50 m, ID = 0.25 mm) and the 2nd dimension column was a polar BPX-5 column (2 m, ID = 0.15 mm). The effluent from GC x GC separation was analyzed by FID for product quantification. The FID response was determined by dosing different amounts of iso-butane (5%, balance He). For some tests, fluoranthene was used as an additional internal standard, which was loaded downstream the catalyst, separated by a plug of quartz wool, allowing the fluoranthene to desorb without contacting the catalyst upon heating the catalyst reactor under He flow [69]. GC Image software was used for data processing and based on the FID response for the internal standard the yields of all other products was calculated using the effective carbon number approach [70]. For selected tests, a BenchTOF-Select™ (Markes, United Kingdom) was used utilizing a scanning range of m/z = 20–600 at 70 eV to identify the products spectra with the NIST library database (MS search 2.2).

The mass closure for non-catalytic tests was relatively low (~55 wt%) since only light waxes could be quantified with the GC while heavy waxes (>C_{36}) were outside the GC range. For catalytic

upgrading, higher mass closures in the range of 80-110% resulted. Since no or only minor amounts of light waxes up to C_{35} were detected when using the catalysts, for a better comparison the yields from catalytic tests were normalized without taking into account potentially minor amounts of heavy waxes (outside the GC range) and catalytic coke, which was determined to be minor (~1 wt% or lower) for all catalysts.

2.4 Test Conditions

2.4.1 Yield Tests

0.4±0.02 mg of LDPE (<300 µm) was pyrolyzed at a fixed pyrolysis temperature of 550 °C. A constant bed volume was maintained by dilution with low-surface area α-Al_2O_3 (0.04 m^2/g, Final Advanced Materials Sàrl) to maintain a constant contact time despite differences in catalyst loading and density. Thermal reference tests were performed using the bare α-Al_2O_3 without catalyst at the upgrading temperatures of 600 and 700 °C investigated in this work. Catalyst loadings of 16, 32, and 60 mg were investigated, corresponding to catalyst/feed ratios of 40, 80, and 150.

2.4.2 Deactivation Tests

To study the deactivation of the steamed and unsteamed version of the high HZSM-5 additive by coking, MPO (see section 4.1) was used as feed. Similar to previously described single experiments with LDPE, 0.4±0.02 mg accurately weighed and pyrolysis at 550 °C with the catalyst reactor operated at 700 °C. The deactivation was achieved by repeatedly passing pyrolysis pulses over the catalyst, thereby simulating a continuous feeding. In order to accelerate the deactivation investigation, a full GC × GC analysis was only performed after every ~25th or 50th pyrolysis vapor pulse. For the pyrolysis vapor pulses in between these full GC × GC analyses, the catalyst was maintained at its working temperature, but a shortened GC oven program was run that maintained the oven at 150 °C during the reaction and then quickly heated the GC oven to 320 °C to clean the columns. The deactivation study was performed using 60 mg of the steamed catalyst and 6 mg of

the unsteamed catalyst due to the much higher activity of the unsteamed version. In total, 155 × 0.4±0.02 mg of pyrolysis vapors from the MPO feed were passed over each catalyst.

3 RESULTS

3.1 Feed Properties

The virgin LDPE feed contained C (85 wt%) and H (15 wt%), similar to what has been reported by other researchers for LLDPE (85.8 wt% C and 14.2 wt% H) [71]. On the other hand, the cold-washed MPO contained appreciable amounts of N and O. The origin of these heteroatoms are attributed to N-containing polyamide and O-containing PET contaminations in the MPO. In addition, there were apparent differences between the virgin PE and the MPO in terms of their volatiles, fixed carbon, and ash/inorganics content. While virgin PE contains no fixed carbon and ash—in line with observations by others [19]—the MPO comprised 0.3 wt% fixed carbon and 2.8 wt% ash (**Table 3**, Fig. S2). The higher content of fixed carbon compared to the virgin PE sample could have resulted from contamination with Carbon Black filler material since the pellets were dark grey; in addition, the contained PET contamination has a high tendency for the formation of fixed carbon formation with values of ~18 wt% reported [71] and also PS has a higher coking potential compared to PE/PP [72,73]. The MPO ash was white and visible when subjecting a larger sample amount to calcination at 600 °C in a muffle furnace (**Figure 1**). The ash-test in a muffle furnace and the proximate analysis using TGA indicated the same level of inorganics (2.8 wt%).

Table 2. Elemental composition on an inorganics-free basis.

	C %	H %	N %	O %
LDPE	85.7[a]	14.3[a]	0	0
MPO	83.7 ±0.22[b]	14.2 ±0.12[b]	0.35 ±0.03[b]	1.71 ± 0.21[b]

[a]Due to the high purity of the virgin sample, the elemental compositions was calculated based on its molecular formula; [b]standard deviation from ninefold analysis

Table 3. Analysis of volatiles, fixed carbon, and inorganics content

	LDPE	MPO
Volatiles (wt%)	100	96.9
Fixed carbon (wt%)	0	0.3
Ash (wt%)	0	2.8

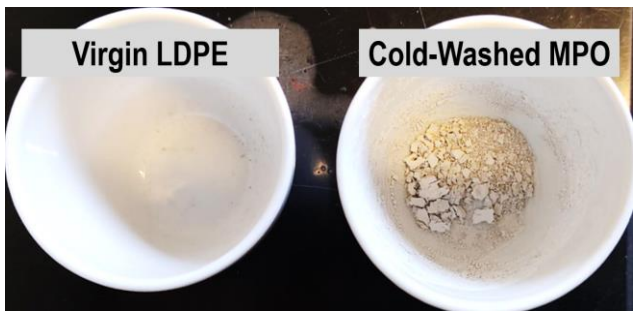

Figure 1. Inorganics remaining after heating ~4 g of ground sample to 600 °C in the muffle furnace

3.2 Catalyst Properties

Table 4 summarizes the textural properties, chemical composition, and acidity of the different steamed catalysts. The catalysts had an apparent bulk density of 0.7-0.8 and a Davison Index, which is a measurement of attrition rate between 2 and 5. The HZSM-5 additives contained ~13 wt% P_2O_5 and the FCC formulations contained ~2 wt% rare earth oxides (RE_2O_3). FCC formulation D had about twice as much matrix surface area than the FCC formulation C, and a four times higher ratio of zeolite surface area to matrix surface area (Z/M). The latter ratio is an important parameter to determine how much of the cracking is done by the external vs. internal acid sites.

The total acidity of the steam-treated catalysts can be regarded as fairly low; e.g., the high HZSM-5 content additive had only about ~10% of the acidity observed in a freshly calcined pure HZSM-5 (Si/Al ~40) [56]. This can to some extent be explained by the dilution of zeolite in the

less acidic matrix, but mostly, to the high-severity hydrothermal treatment, which decreases the acidity of the zeolite component via dealumination [36,74]. As a result, the acidity of the high HZSM-5 content additive decreased to 15% acidity of its initial acidity (Table 4). The steamed FCC formulations had a higher acidity of 0.08-0.13 mmol NH_3/g compared to the steamed HZSM-5 additives (0.03-0.06 mmol NH_3/g). In this regard, it is worth noting that the FCC catalyst formulation contained rare earth (La), since the stabilizing La3+ ions prevent dealumination of the zeolite Y component in the FCC catalysts [75].

From the desorption profiles (Figure S3) and the contribution of acid sites with different strength determined by Gaussian peak fitting (Table S1), it can be seen than all steamed catalysts have a high contribution (>80%) of very weak (NH_3 desorption at ~175 °C) and weak (NH_3 desorption at ~250 °C) acid sites. For the steamed HZSM-5 additives, ≥95% comprise very weak and weak acidity, while the FCC and E-Cat very weak and weak acidity make up 84-86% of the catalysts' acidity. The unsteamed HZSM-5 additive showed the highest proportion (22%) of medium and strong acid sites. Olazar et al. [52] reported that the FCC catalyst that was steamed at similar temperature (816 °C) but slightly longer (8h) than in the present work (4h at 815 °C) had only 7% of the acidity of the fresh FCC catalyst. As expected, amongst the steamed catalysts used in the present work, the additive with the higher ZSM-5 content in the formulation showed a higher acidity (0.056 mmol NH_3/g) compared to the lower HZSM-5 content additive (0.034 mmol NH_3/g). In addition, the surface area was higher for the additive with the higher HZSM-5 content. This demonstrates that despite the high-severity steaming, the phosphorus-stabilized zeolite did not lose activity completely since a complete amorphization, i.e., loss in crystallinity, would have resulted in a loss of microporosity and therefore surface area [36,37,41,76].

Table 4. Catalyst properties

	Al_2O_3	Na_2O	P_2O_5	RE_2O_3	Surface area	Matrix surface area (M)	Zeolite surface area (Z)	Z/M	Acidity[c]
	wt%	wt%	wt%	wt%	m^2/g	m^2/g	m^2/g	-	mmol NH_3/g
Steamed additive A (medium ZSM-5 content)[a]	27.5	0.11	12.6	-	140	n.d.	n.d.	n.d.	0.03
Steamed additive B (high ZSM-5 content) [a]	19.8	0.07	13.3	-	198	n.d.	n.d.	n.d.	0.06
Unsteamed Additive B [a]	21.4	0.05	13.5	-	180	n.d.	n.d.	n.d.	0.40
Steamed FCC formulation C [a]	46.8	0.3	-	1.98	203	39	164	4.2	0.08
Steamed FCC formulation D [a] (higher matrix SA)	50.4	0.29	-	1.99	180	84	96	1.1	0.13
E-Cat (FCC+HZSM-5 additive)[b]	n.d.	n.d.	n.d.	n.d.	153	28[d]	126[d]	n.d.	0.07

[a]provided by W.R. Grace & Co.-Conn, [b]provided by TotalEnergies after refinery operation, [c]NH_3-TPD profiles provided in the supplemental information, Fig. S3 [d]by *t-plot* method from N_2 physisorption data

3.3 Product Yields

3.3.1 Non-Catalytic Conditions

The pyrolysis temperature in the present work was 550 °C, since pyrolysis temperatures of 500 °C or lower lead to significantly broader volatilization profiles (Fig. S1). For LDPE and MPO feed, three thermal reference tests were carried out: i) operating the upgrading reactor empty at a temperature of 375 °C, high enough to avoid condensation of heavy vapor phase waxes and low enough to initiate thermal cracking, and ii) and iii) replacing all catalyst with α-Al_2O_3 and operating the reactor at 600 °C and 700 °C, respectively. Compared to operating the reactor empty, at 600 °C with α-Al_2O_3 there was an increased contribution of C_1-C_4 light products and aromatics. As expected, the thermal cracking effect was more pronounced when increasing the upgrading reactor temperature to 700 °C. Similar observations were made using MPO as feed; however, the higher yield of aromatics compared to using LDPE as feed is noteworthy (**Table 5**). This is attributed to PET and PS contamination, e.g., when operating the second reactor empty at 375 °C the styrene yield was 1.1 wt%. Using MPO as feed and maintaining α-Al_2O_3 at 600 °C produced 1.1 wt% CO_2, 0.3 wt% CO and 0.04 wt% H_2. The presence carbon oxides is attributed to the deoxygenation of PET, with a higher extent of decarboxylation over decarbonylation [19]. In addition, typical products from the pyrolysis of PP [77–80] could be detected, such as 2,4-

Dimethyl-1-heptene (1.7 wt%), explaining a higher fraction of C_5-C_{11} compared to LDPE. As expected from the presence of heteroatoms indicated by the elemental analysis, also oxygen and nitrogen-containing products we detected amongst the pyrolysis products. Examples include benzophenone and caprolactam (1.2 wt%), the latter being clear evidence of the polyamide contamination [79] in the mixed polyolefin feed. Other compounds include squalene and Cholesta-3,5-diene, the former likely being a residue from cosmetic products or used as additive, e.g. squalene was found in PP [81]. Lastly, a few long chain (C_{14}-C_{18}) acids, nitriles, and amides were detected, likely stemming from various animal and vegetable fats and oils or used as additives [81], which due to their low solubility in water were not removed by the cold-washing pretreatment.

Coke was below the detection limit for tests with α -Al_2O_3, and similarly, H_2 yield was very low (0.03 wt%). For catalytic tests at 600 °C, the hydrogen yield increased to ~0.1 wt% (from 0.03 wt% with α-Al_2O_3), and for tests at 700 °C it further increased to ~ 0.3 wt%. H_2 yields often correlate with the yields of coke and aromatics (=coke precursors) due to their lower H/C ratio compared to the feed.

It has to be acknowledged that the mass closure for non-catalytic tests was only ~55 wt%. This can be attributed to the fact that only the light waxes could by quantified with the GC while heavy waxes (>C_{36}) were outside the GC range. Estimating the yield of C_{21+} waxes at a pyrolysis temperature of 550 °C by difference in the mass balance closure indicates about 60 wt% C_{21+} waxes, which agrees with reports by other researchers stating ~50 wt% at 600 °C and ~69 wt% at 500 °C (75 wt% for PP) [82].

Table 5. Yields (wt%) of main products from non-catalytic pyrolysis of LDPE and MPO at a pyrolysis temperature of 550 °C and different thermal reference conditions for the upgrading reactor.

feed	Upgrading reactor	Upgrading reactor Temperature [°C]	CH_4	C_2-C_4 olefins	Ethylene	Propylene	1,3-Butadiene	Other C_4=	Aromatics (PAH)[b]	Aromatic-free C_5-C_{11}	C_{12}-C_{20}	C_{21}-C_{35} (measured)	C_{21+} (by difference)
LDPE	Empty	375	0.2	2.9	1.0	1.1	0.2	0.6	0.0 ()	13.1	24.0	14.6	60
	α-Al_2O_3	600	0.4	7.7	3.0	2.5	0.5	1.3	2.8 ()	12.3	19.5	29.8	57
	α-Al_2O_3	700	1.1	29.8	12.9	7.7	3.0	6.0	2.9 ()	21.6	13.0	8.7	31
MPO	Empty	375	0.5	2.9	0.9	1.2	0.2	0.6	1.9 ()	17.7	16.0	14.9	58
	α-Al_2O_3 [a]	600[a]	0.6	9.3	3.0	3.0	0.7	1.7	5.0 ()	15.5	22.3	32.8	45
	α-Al_2O_3	700	0.9	30.4	11.1	8.8	3.0	6.4	5.4 ()	24.6	17.5	12.8	20

[a]under these conditions, 1.1 wt% CO_2, 0.3 wt% CO and 0.04 wt% H_2 were produced; [b]number before the brackets shows the total yield of aromatics, i.e., monoaromatics + polyaromatic hydrocarbons, and the yield in brackets indicates the yield of polyaromatic hydrocarbons

3.3.2 Catalytic Cracking at Moderate Severity

At a catalyst/feed ratio of 40:1 and a catalyst temperature of 600 °C, there was a clear effect of the catalysts on the product distribution compared to the thermal reference using pure α-Al_2O_3; particularly, a shift towards lighter products , and a significant increase in the yields of C_2-C_4 olefins and aromatics (**Table 6**) was observed. The definition of C_2-C_4 olefins includes ethylene, propylene, C_4 butenes (iso-butene/1-butene, and cis/trans 2-butene), and 1,3-butadiene. CH_4 yields were low for all catalysts (≤0.5 wt%), indicating that thermal and catalytic over-cracking was still limited at 600 °C, likely due to the low acidity and absence of very strong acid sites in the steamed/equilibrated catalysts. The additive with high HZSM-5 content showed the highest C_2-C_4 olefin selectivity of 53 wt%, while only 41 wt% was obtained with the medium ZSM-5 content additive. The increased activity of steamed additive B (high ZSM-5 content) compared to steamed additive A (medium ZSM-5 content) can be reasonably explained by the higher number of acid sites of additive B (0.06 NH_3/g) compared to additive A (0.03 NH_3/g).

The FCC catalyst formulations obtained a higher yield of C_5-C_{11} aliphatics than the additives, with maximum values of ~42 wt% achieved using the FCC formulation with a higher matrix surface area. The FCC formulations generally showed higher conversions of the larger C_{12+} products compared to the HZSM-5 additives. FCC catalysts are designed for converting large molecules present in crude oil. The Y-zeolite component in FCC catalysts is known to have a larger pore opening of 0.8 nm compared to ZSM-5 (0.5 nm). In addition, steaming of the FAU type Y zeolite at high temperatures can create mesoporosity in the Y-zeolite while steaming does not lead to appreciable creation of mesopores in ZSM-5 [83,84]. As a result, the pore structure of FCC catalysts may have allowed for better accessibility and conversion of waxes compared to the HZSM-5 additives. In addition to differences in pore size distribution, the steamed FCC formulations had a higher acidity of 0.07-0.13 mmol NH_3/g compared to the steamed high HZSM-

5 content additive with 0.06 mmol NH_3/g (**Table 4**). Therefore, the improved conversion of larger C_{12+} aliphatics may be the combined result of better accessibility and the higher number of acid sites available for reaction.

A physical mixture of the Grace FCC catalyst and the HZSM-5 additive produced ~2 wt% more light olefins (predominantly propylene) and ~5 wt% more aromatics than the yields expected theoretically based on the product distribution obtained with the bare catalysts (**Table 4**). Mixing of FCC catalyst and HZSM-5 additive may have allowed synergetic effects favoring aromatization reactions. This is, because the FCC catalyst is more effective in converting the larger molecules to smaller ones, but it does not contain pore sizes that are selective for the formation of monoaromatics. Large molecules have difficulties diffusing into the shape-selective micropores of the ZSM-5 additives, and therefore, the pre-cracking of the larger molecules with the more acidic FCC catalyst formulations in the mixture seemed helpful to produce smaller molecules that could diffuse into the micropores of the ZSM-5 additive and undergo aromatization reactions. This is also supported by the observation that the yield of propylene, an important product from the hydrocarbon-pool mechanism [85–87], was 2.0 wt% higher with the physical mixture compared to what would have been expected theoretically based on using the bare HZSM-5 additive B and FCC formulation C. The observations are in line with high yields of aromatics obtained with the E-Cat, which is a physical mixture of FCC catalyst and 5-10% HZSM-5 additive. Doubling the amount of E-cat catalyst loading increased the C_2-C_4 olefins yield from 45 to 47 wt% and the aromatics yield from 11 to 16 wt% while decreasing the yield of products in the C_5-C_{20} fraction, suggesting that these higher products were further catalytically cracked to C_2-C_4 olefins. Importantly, the increased catalyst contact time did not lead to a marked increase in CH_4, which again is attributed to the low acidity of the equilibrated catalyst compared to a fresh one.

While HZSM-5 is known to favor aromatization based on its pore size, it is interesting to note that the FCC catalysts obtained higher yields of aromatics compared to the HZSM-5 additives, both at 600 °C and even more so at 700 °C (next section). Possible explanations for this observation could be the higher acidity of the FCC catalysts compared to the HZSM-5 additives (**Table 4**), and that there was an important effect of pre-cracking the larger molecules in the matrix. The high ZSM-5 additive may have produced less aromatics compared to the medium ZSM-5 content additive because for the same catalyst loading less matrix was available to pre-crack the vapors and the uncracked chains could not diffuse into the pore channels of the catalyst. The higher yields of C_{12+} products compared to the medium ZSM-5 content catalyst further support this theory (**Table 6** and **Table 8**). In addition, the coking propensity tends to correlate with higher yields of aromatics since they are coke precursors. Generally, higher coke yields resulted from using the FCC catalysts and it is well known that the Y-zeolite contained in FCC catalysts contains a high density of acid sites, active for cracking and aromatization. In addition, even the matrix component itself was shown to be active for aromatization [27].

With respect to functionalities of higher straight chain aliphatics, the catalytic upgrading significantly decreased the yield of α-olefins and diolefins with the unsaturation in the alpha and end position (ω) compared to the thermal reference case (**Figure 2**). A comparison of the C_{12}-C_{27} functionalities summarized in **aC2-C4 olefins** includes ethylene, propylene, C_4 butenes (=sum of iso-butene/1-butene, and cis/trans 2-butene), and 1,3-butadiene; [b]number before the brackets shows the total yield of aromatics, i.e., monoaromatics + polyaromatic hydrocarbons, and the yield in brackets indicates the yield of polyaromatic hydrocarbons

Table 7 shows that di-olefins were converted completely, and also the yield of alpha-olefins was severely reduced from 15 wt% (thermal) to 1-2 wt% with the different catalysts. A minor difference was observed for the yield of n-paraffins, with ~1 wt% higher yields using the HZSM-5 additives and ~2 wt% lower yields using the different FCC catalyst formulations. The observation can be explained by the higher reactivity of α-olefins and dienes since the unsaturation at the end of the chain provides high electron density and little steric limitations, thereby facilitating their reaction with protonated acid sites, followed by the formation of carbocations and beta-scission. Alkanes may potentially also result from hydrogen transfer reactions; however, since the combined yield of iso-butane and n-butane was fairly low (≤1 wt%) compared to the yield of C_4 olefins (16-22 wt%), the extent of hydrogen transfer is deemed minor.

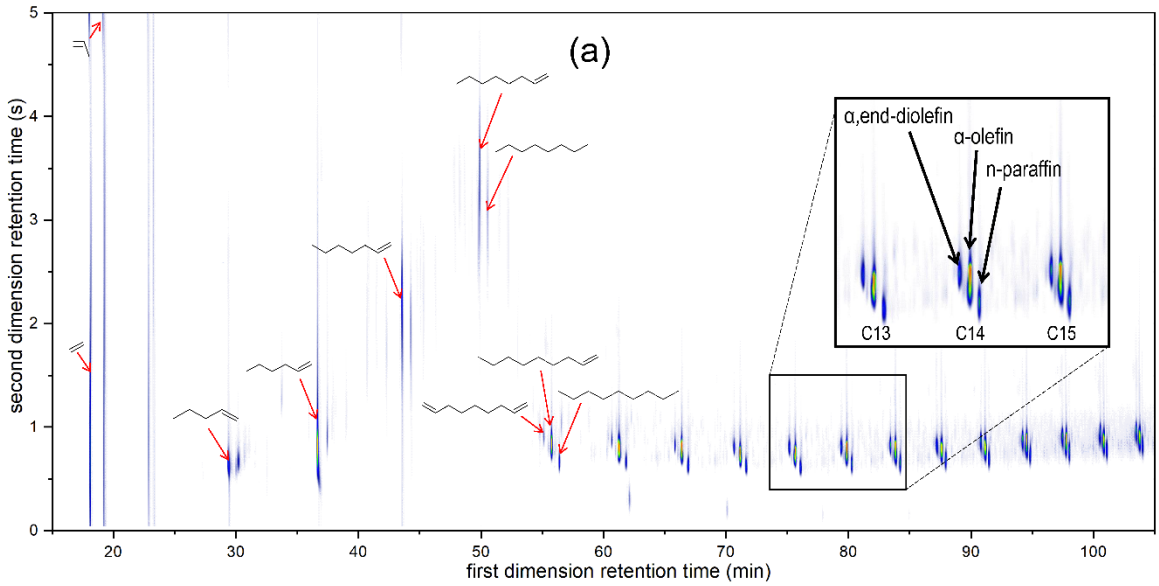

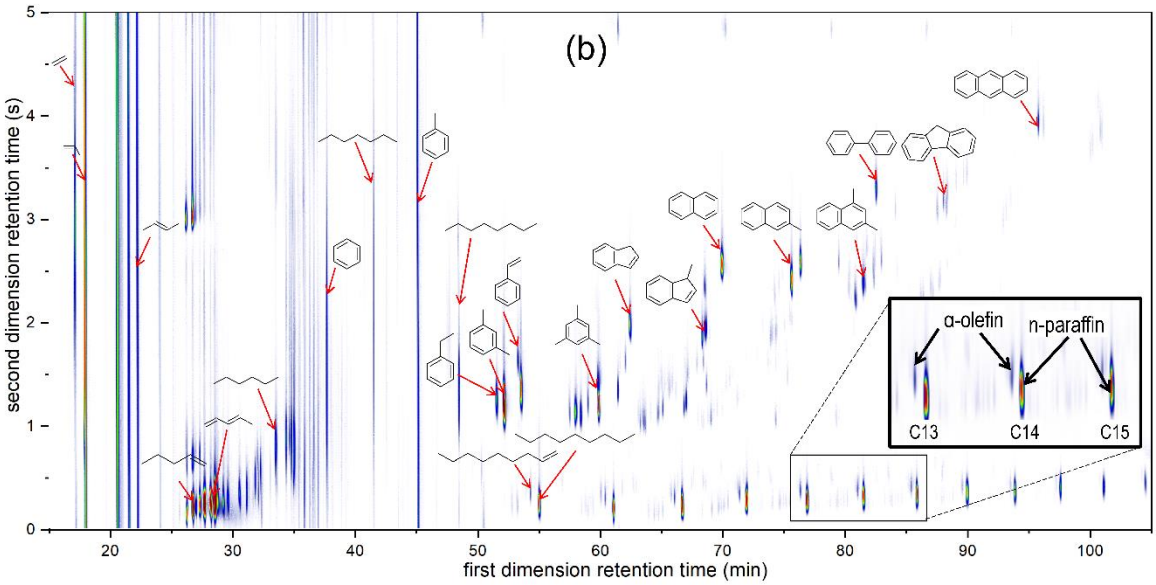

Figure 2. Products obtained from passing LDPE pyrolysis vapors over (a) α -Al_2O_3, and (b) E-cat (=FCC + HZSM-5 additive) at 600 °C.

Table 6. Yields (wt%) obtained for a single run at a catalyst temperature of 600 °C using virgin LDPE as feed for the pyrolysis reactor (550 °C)

Catalyst	catalyst/feed ratio	cumulative feed/catalyst	CH_4	C_2-C_4 olefins[a]	Ethylene	Propylene	1,3-Butadiene	Other C_4=	C_4 Alkanes	Aromatics (PAH)[b]	Aromatic-free C_5-C_{11}	C_{12}-C_{20}	C_{21}-C_{35}
Steamed additive A (medium ZSM-5 content)	40	0.025	0.5	40.4	4.3	18.5	1.3	16.3	0.8	10.9 (1.6)	28.1	15.9	3.4
Steamed additive B (high ZSM-5 content)	40	0.024	0.4	50.6	5.3	24.2	1.6	19.5	0.8	6.6 (0.9)	23.9	14.7	3.0
Steamed FCC formulation C	40	0.024	0.3	34.7	2.4	13.3	0.5	18.5	0.9	12.3 (1.7)	41.6	8.6	1.6
Steamed FCC formulation D (high matrix SA)	40	0.024	0.4	37.9	2.8	14.2	1.1	19.8	0.6	10.6 (1.1)	42.5	7.7	0.2
Steamed FCC formulation C + Steamed additive B	40	0.024	0.3	44.6	4.0	20.5	1.0	19.1	1.0	14.4 (2.6)	30.6	8.2	0.9
E-Cat (FCC+HZSM-5 additive)	40	0.025	0.4	45.4	2.9	19.5	0.9	22.1	0.5	10.9 (1.1)	36.4	6.1	0.4
E-Cat (FCC+HZSM-5 additive)	80	0.012	0.4	47.0	3.6	21.2	1.2	20.9	1.0	16.0 (2.6)	28.8	5.9	1.0

[a]C_2-C_4 olefins includes ethylene, propylene, C_4 butenes (=sum of iso-butene/1-butene, and cis/trans 2-butene), and 1,3-butadiene; [b]number before the brackets shows the total yield of aromatics, i.e., monoaromatics + polyaromatic hydrocarbons, and the yield in brackets indicates the yield of polyaromatic hydrocarbons

Table 7. Yields of C_{12}-C_{27} α,ω-diolefins, α-olefins, and n-paraffins obtained for a single run at a catalyst/feed ratio of 40:1 and catalyst temperature of 600 °C using virgin LDPE as feed for the pyrolysis reactor (550 °C).

Catalyst	**Yield of C_{12}-C_{27} α,ω-diolefins (wt%)**	**Yield of C_{12}-C_{27} α,olefins (wt%)**	**Yield of C_{12}-C_{27} n-paraffins (wt%)**
α-Al_2O_3	6.5	14.7	6.7
Steamed additive A (medium ZSM-5 content)	0	1.8	7.6
Steamed additive B (high ZSM-5 content)	0	1.4	7.8
Steamed FCC formulation C	0	1.1	4.7
Steamed FCC formulation D (high matrix SA)	0	1.0	4.8
E-Cat (FCC + HZSM-5 additive)	0	0.8	5.1

3.3.3 Catalytic Cracking at High Severity

Increasing the catalytic cracking severity by increasing the catalyst/feed ratio from 40:1 to 150:1 and the catalyst temperature from 600 to 700 °C further shifted the product distribution to lighter products (**Figure 3**) and led to 2-4 times higher yields of CH_4 (**Table 8**) using the steamed FCC and HZSM-5 additives. Even higher CH_4 yields of 2.7 wt% resulted using the E-Cat. This can be attributed to a greater extent of "overcracking" and possibly also to an increased content of metals such as nickel, vanadium and sodium that had accumulated on the E-Cat from upgrading fossil feed in the refinery operation. This is also indicated by the fact that not only the C_{12}-C_{20} compounds, still present at appreciable yields at the lower cracking severity (**Table 6**), were significantly reduced, but there was also an apparent decrease in the C_5-C_{11} aliphatics fraction, especially when using the FCC catalysts (**Table 8**).

This higher activity of the FCC catalysts for converting the more difficult to crack C_5-C_{11} aliphatics is likely a result of their higher acidity compared to the HZSM-5 additives (Table 4). For both HZSM-5 additives and FCC catalysts, the higher cracking severity conditions allowed to boost the yield of C_2-C_4 olefins by an additional ~16 wt%, while at the same time also the yield of aromatics increased by 4-12 wt% (**Table 6** and **Table 8**). In the carbon number (C#) distribution shown in (**Figure 3**), this is visible by the high contributions of C# = 7 (toluene) and C# = 10 (naphthalene and alkylated benzenes) at the increased catalytic temperature. Within the C_2-C_4 olefin fraction, particularly the yield of ethylene saw the most substantial increase by more than 10 wt% (**Figure 3**). An increase in aromatics with higher temperatures was also observed by Artetxe *et al.* [88] for inline upgrading of HDPE-derived

pyrolysis vapors with an agglomerated HZSM-5 catalyst at 450 and 500 °C, reporting 10 and 12 wt% aromatics, respectively. It is noted that under thermal pyrolysis conditions, increasing the pyrolysis temperature favors the formation of poly aromatic hydrocarbons (PAH) since monoaromatics are precursors to PAH. As an example, Ki-Bum Park et al. [89] reported 16 wt% monoaromatics and 5 wt% PAH at a pyrolysis temperature of 654 °C, and 13 wt% monoaromatics and 9 wt% PAH at a pyrolysis temperature of 732 °C using LDPE as the feedstock. For using PP as the feedstock, the yield of monoaromatics increased from 10 to 13 wt% and the yield of PAH increased from 2 to 12 wt% when increasing the pyrolysis temperature from 621 to 768 °C [90]. In the present work, at a catalyst temperature of 600 °C, the proportion of PAH in the aromatics yield was 10-18% for the different catalysts (**Table 6**), and it was 3-13% at a catalyst temperature of 700 °C (**Table 8**). This suggests that the extent of condensation of monoaromatics to PAH was minor, likely due to the short catalyst contact time and absence of strong acid sites (Figure S3, Table S1).

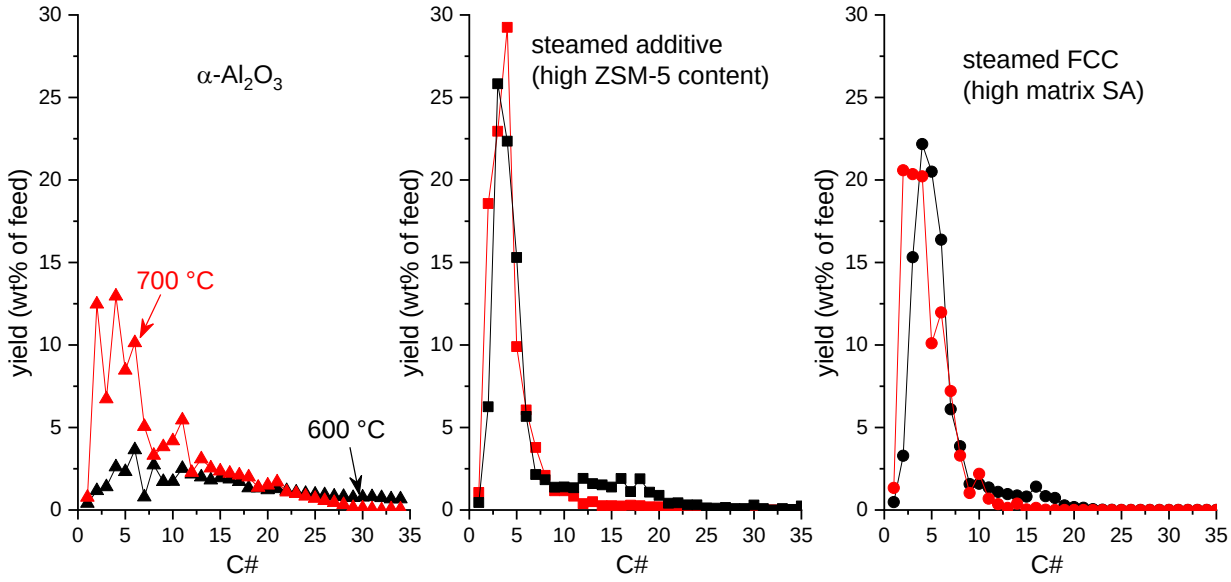

Figure 3. Carbon number (C#) distribution from upgrading LDPE-derived pyrolysis vapors over α-Al_2O_3, steamed additive with high ZSM-5 content, and steamed FCC with high matrix SA at a catalyst temperature of 600 °C (black) and 700 °C (red).

Table 8. Yields (wt%) obtained for a single run at a catalyst temperature of 700 °C and a catalyst/feed ratio of 150:1 using virgin LDPE as feed for the pyrolysis reactor (550 °C)

Catalyst	CH_4	C_2-C_4 olefins[a]	Ethylene	Propylene	1,3-Butadiene	Other C_4=	C_4 alkanes	Aromatics (PAH)[b]	Aromatic-free C_5-C_{11}	C_{12}-C_{20}	C_{21}-C_{35}
Steamed additive A (medium ZSM-5 content)	0.9	57.3	14.8	23.3	6.0	13.1	0.6	15.7 (1.8)	20.3	3.4	1.8
Steamed additive B (high ZSM-5 content)	1.1	69.3	18.5	22.3	10.4	18.1	0.2	11.8 (1.4)	14.5	2.6	0.6
Steamed FCC formulation C	2.1	49.3	10.0	14.8	6.6	17.9	1.0	23.2 (2.9)	22.6	0.9	0.8
Steamed FCC formulation D (high matrix SA)	1.3	58.2	20.2	19.4	7.3	11.3	0.9	22.6 (3.0)	16.1	1.0	0.0
E-Cat	2.7	69.1	22.9	30.7	4.1	11.4	1.1	18.6 (0.6)	6.9	1.2	0.3

[a]C_2-C_4 olefins includes ethylene, propylene, C_4 butenes (=sum of iso-butene/1-butene, and cis/trans 2-butene), and 1,3-butadiene

3.4 Deactivation Tests for HZSM-5 Additive

At both moderate and severe cracking conditions, the additive with high HZSM-5 content obtained the highest yield of C_2-C_4 olefins (see Table 6 and Table 8), closely followed by the E-Cat. Therefore, the change in product distribution during deactivation was studied further using the HZSM-5 additive. MPO was used as a feed instead of virgin LDPE since MPO is more relevant from an industrial point of view and more coking was expected using MPO instead of the virgin PE feed. This is mainly due to the contamination with other plastics such as PET and PS, which have a higher coking potential compared to PE/PP [72,73]. Since the steaming pretreatment had severely reduced the catalyst's acidity (**Table 4**), the comparison was deemed fairer by lowering the catalyst loading of the fresh catalyst to 6 mg so that a similar initial conversion of C_{12+} products was obtained compared to using 60 mg of steamed catalyst (**Figure 4**b and d). When an increasing amount of pyrolysis vapors was processed over the steamed catalyst, a sight decrease in ethylene (from 22-19 wt%) and propylene (from 31 to 26 wt%) resulted (**Figure 4**a). For the unsteamed catalyst (**Figure 4**c), the decrease in ethylene was less pronounced (21 to 18 wt%) compared to the decrease in propylene (25 to 17 wt%). This is attributed to the fact that at 700 °C, a reasonably high contribution (~12 wt%) of total ethylene yield is attributed to thermal cracking, while only ~7 wt% of propylene was produced under thermal cracking and therefore the decline in propylene yield due to catalyst deactivation was more pronounced. Similarly, for the unsteamed catalyst, the decline in butadiene yields was minor (from 6.5 to 5.3 wt%) due to a high contribution of butadiene from thermal cracking while the decline in 1-butene/isobutene yield (combined peak in chromatogram) was more pronounced. Interestingly, for the steamed catalyst, the yield of other C_4 olefins (1-butene/isobutene, and cis/trans 2-butene) increased slightly initially, before decreasing eventually at a high run number of ~160, while the yield of aromatics appeared to show the opposite trend (**Figure 4**a). Similarly, the yield of propylene increased slightly from ~30 wt% for

run #1 to 31 wt% for run #27 and #55 before eventually starting to decline (run #104, 28 wt%; run #157, 26 wt%). This observation may be attributed to coking.

While for steamed and unsteamed catalysts the yield of aromatic-free C_5-C_{11} compounds increased with an increasing amount of vapors processed over the catalyst, the unsteamed catalyst produced about twice as much C_5-C_{11} aliphatics compared to the steamed version. This may result from stronger acid sites present in the unsteamed version, active in trans alkylation and isomerization (Table S1). The aromatics yield was higher using the steamed catalyst, while it was fairly low ~5 wt% and constant using the unsteamed version. Importantly, the steamed catalyst showed fairly constant conversion of C_{12}-C_{35} products, while there was a evident decline in the conversion of C_{12}-C_{35} products observed using the fresh catalyst (**Figure 4**b vs. d). This is attributed to the higher coking rate using the fresh catalyst.

The quantification of the coke that had accumulated on the steamed and unsteamed catalysts corresponded to a coke yield of 0.74 wt% and 0.12 wt%, respectively. At first it may seem unexpected that the unsteamed catalyst had lower coke yields owing to its higher acidity, but it should be kept in mind that the catalyst loading was only $1/10^{th}$ of the steamed catalyst. For the steamed and the unsteamed versions, the coke load per coke-free catalyst [w/w] amounted to 0.008 and 0.012, and the coke load per catalyst surface area was 40 $\mu g/m^2$ and 68 $\mu g/m^2$, respectively. This shows that the unsteamed catalyst had a 71% higher coking propensity. This higher coking propensity is expected based on the overall higher acidity of the unsteamed catalyst and its higher content of medium-strong acid sites (**Table 4**, Table S1). This comparison assumed that the carbon deposition on the α-Al_2O_3 used as diluent can be neglected since the surface area of the diluent in the fixed bed amounted to less than 1% of the catalyst surface area.

With the progressed loss in activity due to coking observed for the unsteamed catalyst, particularly the yield of higher α-olefins and α,end-diolefins increased (**Figure 5**). Note that the chromatographic method only allowed a proper separation between dienes, α -olefins, and paraffins until C_{27}.

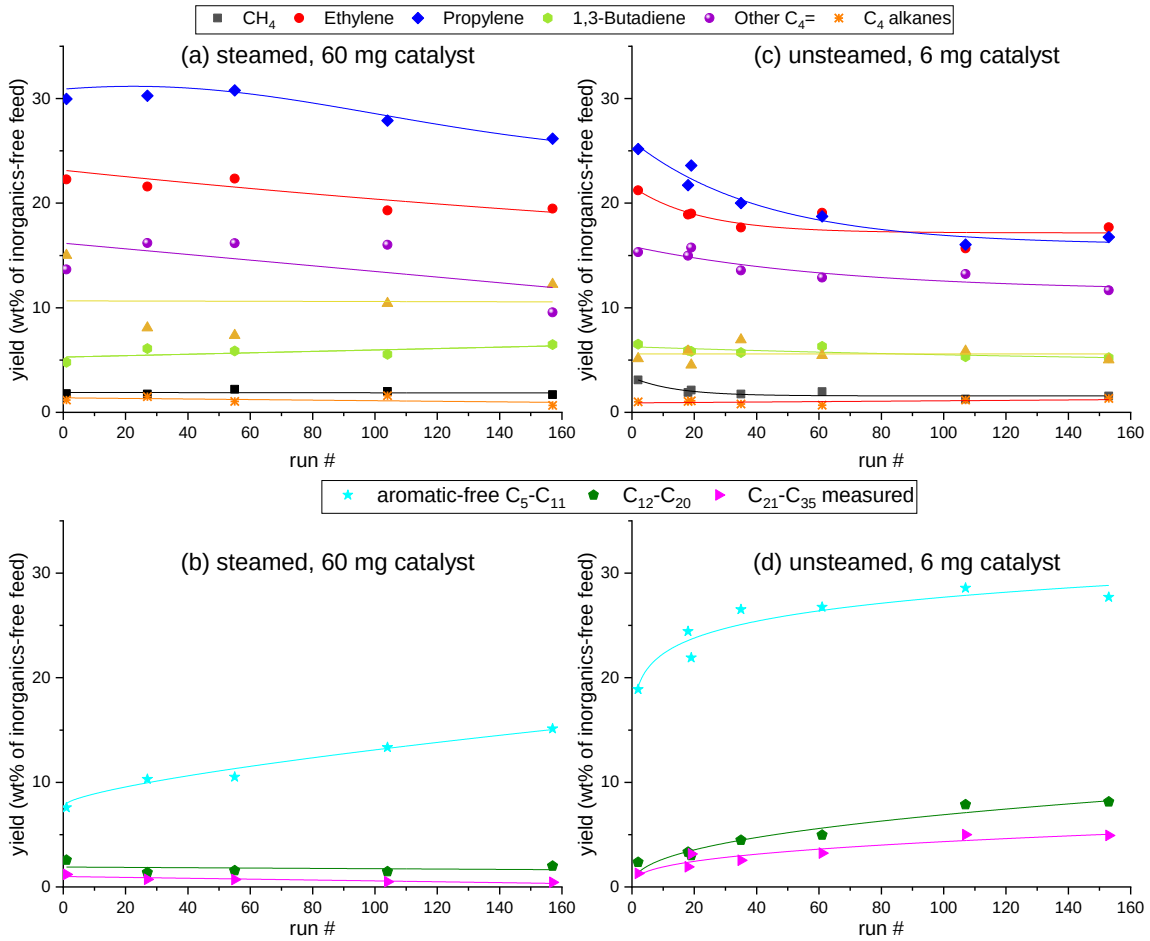

Figure 4. Product yield profiles as function of the number of catalytic pyrolysis tests: (a) and (b) steamed, and (c) and (d) unsteamed. One run # corresponds to 0.4 mg of MPO being pyrolyzed. Yields are shown based on inorganics-free feed. The fitted lines are guides to the eye.

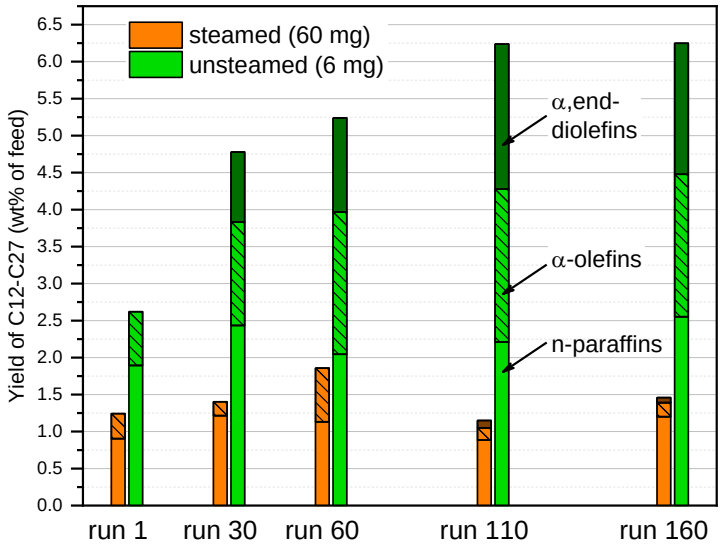

Figure 5. Yields of C_{12}-C_{27} dienes, α-olefins, and paraffins. Minor yields of beta-olefins, iso-olefins/paraffins at much lower selectivities compared to the three main product groups not shown.

4 DISCUSSION

Commercially it is of interest to maximize propylene yields and this is often achieved by utilizing additives and/or increasing the severity of the process by increasing the catalyst-to-feed ratio and/or the reaction temperature. To the best of our knowledge, in traditional FCC processing of resid or VGO as feed the yields of propylene hardly exceed ~22 wt% [32,91–93]. In the present work, significantly higher propylene yields were obtained by upgrading pyrolysis vapors from virgin PE and even more so from real post-consumer MPO waste. Under the assumption that the energy demand of a mixed polyolefin pyrolysis-to-light-olefins process is roughly comparable to standard FCC operation, this demonstrates the potential of the technology. The process operates at temperatures lower than naphtha steam cracking and requires fewer processing steps than first producing an intermediate pyrolysis oil, de-contaminating the intermediate oil by multi-stage hydrotreatment, and then steam-cracking it for the production of light olefins and aromatics. While for steam cracking the propylene to ethylene ratio (P/E) ranges from 0-1.4 [94], in the catalytic pyrolysis approach at a catalyst temperature of 700 °C the P/E ranged from 1.0-1.6 for the different

catalysts studied in present work, and at 600 °C the P/E ratio was much higher with values ranging from ~4-6.

Advantageously, the carbon losses to coke and CH_4 are kept low with ~1 wt% each using steamed high HZSM-5 content additives, which is lower compared to what has been reported for E-Cats (**Table 1**) and much lower compared to steam cracking. Considering optimistic efficiencies of 80% + 75% for pyrolysis and steam cracking steps starting from sorted polyolefin waste [95], a maximum monomer recovery of ~60% could be achieved. In contrast, the proposed in-line catalytic upgrading bears the potential to recover ~90% of monomers taking into account the recovered C_2-C_4 olefins, aromatics, and considering that the obtained naphtha range aliphatics could subsequently be fed to a steam cracker to be convert to light olefins and aromatics as well (with 75% efficiency).

In the proposed two-stage pyrolysis-upgrading process, most inorganics contaminants are expected to remain in the char fraction inside the pyrolysis reactor, which can be periodically removed. Even if traces of organometallic inorganics would volatilize, the issue could be addressed by passing the vapors through a hot gas filter and tuning the matrix in FCC-type catalyst formulations to be more robust against inorganic contaminants and trap these. The choice of catalyst and operating conditions offers an excellent flexibility in steering the product distribution; instead of maximizing the recovery of C_2-C_4 olefins, refineries may also opt to steer the process towards the high recovery of aromatics (up to ~23 wt% observed in present work), or aim for a high recovery in naphtha-range aliphatics (up to 42% observed in present work).

5 CONCLUSIONS

Upgrading polyethylene pyrolysis vapors over steam-treated FCC and HZSM-5 additive catalysts at 600 °C clearly decreased the yield of C_{12+} products while increasing the yield of C_2-C_4 olefins (plus ~25-40 wt%), aromatics (plus ~10-15 wt%) and naphtha-range aliphatics (plus ~10-

25 wt%). Advantageously, the yields of CH_4 remained fairly low for all catalysts (<0.5 wt%) and similar compared to thermal reference tests using highly inert α-Al_2O_3. FCC catalyst formulations obtained higher yields of C_5-C_{11} aliphatics (up to 42 wt%) and lower yields of C_{12}+ products compared to the HZSM-5-containing additives, indicating their higher activity for converting heavier products. For a physical mixture of FCC catalyst and HZSM-5 containing additive, higher yields of aromatics (plus ~3 wt%) and light olefins (plus ~5 wt%) resulted compared to what would have been expected theoretically. The highest yield of aromatics (17 wt%) was produced using a refinery E-Cat with 5-10% HZSM-5 additive, while the highest C_2-C_4 olefin selectivity of 53 wt% was obtained using a bare steam-treated additive with high HZSM-5 content. With this catalyst, at higher catalyst loading and temperature (700 °C), the light olefin yield reached almost 70 wt% (18% ethylene, 22% propylene, 10% 1,3-butadiene, and 18% other C_4 olefins). Similarly high light olefin yields with even higher propylene yields of up to 31 wt% could be obtained when processing real post-consumer mixed polyolefin waste instead of virgin PE because of the presence of PP.

Finally, the stability against deactivation was investigated for both the steamed and the fresh HZSM-5 additives, whereby the loading of the fresh catalyst was reduced to obtain a similar initial conversion of C_{12+} products. While the steam-treated HZSM-5 additive showed a slow decline in C_2-C_4 olefins and maintained the conversion of C_{12+} aliphatics, the fresh catalyst deactivated faster, apparent by a more rapid decline in C_2-C_4 (particularly propylene) and a breakthrough of unconverted C_{12+} compounds.

Overall, the research results show a great potential for the in-line upgrading of polyolefin vapors with FCC-type catalyst formulations and bare HZSM-5 additives to recover base chemicals such as C_2-C_4 olefins, aromatics, and naphtha-range aliphatics at high selectivity.

Considering that the pre-steamed and equilibrated catalyst formulations are stable against further exposure to steam at moderate reaction temperatures, introducing steam during the reaction may allow to further reduce coke formation and limit the formation of aromatics, thereby potentially slowing down deactivation by coking. Future investigations should also be directed to study the life-cycle-assessment and techno-economic analysis of the presented single step catalytic conversion of plastic waste for comparison with the energy-intensive steam cracking of pyrolysis-derived liquid.

ASSOCIATED CONTENT

Supporting Information

Figure S1: HDPE volatilization profiles obtained at different pyrolysis reactor temperatures; Figure S2: TGA profile for proximate analysis of MPO feed; Figure S3: NH_3-TPD profiles; Table S1: Contribution of very weak, weak, medium, and strong acid sites determined by Gaussian peak fitting of NH_3 desorption profile;

AUTHOR INFORMATION

Corresponding Author: Kevin.VanGeem@UGent.be; Tel.: +32 9 264 55 97

Author Contributions: The manuscript was written through contributions of all authors. All authors have given approval to the final version of the manuscript.

FUNDING SOURCES

This work was performed in the framework of the Catalisti clusterSBO project WATCH (HBC.2019.0001 "Plastic waste to chemicals"), with the financial support of VLAIO (Flemish Agency for Innovation and Entrepreneurship) and the research leading to these results received funding from the European Research Council under the European Union's Horizon 2020 research and innovation programme / ERC grant agreement n° 818607.

ACKNOWLEDGMENT

We are indebted to Dr. Robert Harding (W.R. Grace & Co.-Conn) for providing steam-treated FCC and Olefins additive catalyst formulations and greatly appreciate his feedback to the manuscript. The authors are very grateful to Ir. Cindy Adam (TotalEnergies) for providing a sample of E-cat containing HZSM-5 additive. We are indebted to Prof. Dr. Kim Ragaert for

providing the cold-washed mixed polyolefin pellets used as feed in present work. We thank PhD student Oğuzhan Akin for assisting in analyzing samples by NH_3-TPD.

ABBREVIATIONS

FCC, fluidized catalytic cracking; FID, flame ionization detection; GC, gas chromatography; PE, Polyethylene; PET, Polyethylene Terephthalate; PP, Polypropylene; PS, Polystyrene; ToF-MS, Time-of-Flight Mass Spectrometry; ID, Inner diameter; LDPE, Low density polyethylene; MPO, Mixed Polyolefin waste; TGA, thermogravimetric analysis; TPD, temperature-programmed desorption;

REFERENCES

[1] G. Faraca, T. Astrup, Plastic waste from recycling centres: Characterisation and evaluation of plastic recyclability, Waste Manag. 95 (2019) 388–398.

[2] K. Ragaert, L. Delva, K. Van Geem, Mechanical and chemical recycling of solid plastic waste, Waste Manag. 69 (2017) 24–58. https://doi.org/10.1016/j.wasman.2017.07.044.

[3] M. Mofijur, S.F. Ahmed, S.M.A. Rahman, S.K.Y.A. Siddiki, A.B.M.S. Islam, M. Shahabuddin, H.C. Ong, T.M.I. Mahlia, F. Djavanroodi, P.L. Show, Source, distribution and emerging threat of micro-and nanoplastics to marine organism and human health: Socio-economic impact and management strategies, Environ. Res. 195 (2021) 110857.

[4] A.J. Martín, C. Mondelli, S.D. Jaydev, J. Pé Rez-Ramírez, Catalytic processing of plastic waste on the rise, Chempr. 0 (2020) 1–47. https://doi.org/10.1016/j.chempr.2020.12.006.

[5] S.D. Anuar Sharuddin, F. Abnisa, W.M.A. Wan Daud, M.K. Aroua, A review on pyrolysis of plastic wastes, Energy Convers. Manag. 115 (2016) 308–326. https://doi.org/10.1016/j.enconman.2016.02.037.

[6] Q. Li, A. Faramarzi, S. Zhang, Y. Wang, X. Hu, M. Gholizadeh, Progress in catalytic pyrolysis of municipal solid waste, Energy Convers. Manag. 226 (2020) 113525. https://doi.org/10.1016/j.enconman.2020.113525.

[7] L.O. Mark, M.C. Cendejas, I. Hermans, The Use of Heterogeneous Catalysis in the Chemical Valorization of Plastic Waste, ChemSusChem. 13 (2020) 5808–5836. https://doi.org/10.1002/cssc.202001905.

[8] R. Miandad, M.A. Barakat, A.S. Aburiazaiza, M. Rehan, A.S. Nizami, Catalytic pyrolysis of plastic waste: A review, Process Saf. Environ. Prot. 102 (2016) 822–838. https://doi.org/10.1016/j.psep.2016.06.022.

[9] G. Lopez, M. Artetxe, M. Amutio, J. Bilbao, M. Olazar, Thermochemical routes for the valorization of waste polyolefinic plastics to produce fuels and chemicals. A review, Renew. Sustain. Energy Rev. 73 (2017) 346–368. https://doi.org/10.1016/j.rser.2017.01.142.

[10] D. Hong, P. Li, T. Si, X. Guo, ReaxFF simulations of the synergistic effect mechanisms during co-pyrolysis of coal and polyethylene/polystyrene, Energy. 218 (2021) 119553.

[11] M.S. Abbas-Abadi, K.M. Van Geem, J. Alvarez, G. Lopez, The pyrolysis study of polybutadiene rubber under different structural and process parameters: comparison with polyvinyl chloride degradation, J. Therm. Anal. Calorim. (2021) 1–13.

[12] L. Fan, Z. Su, J. Wu, Z. Xiao, P. Huang, L. Liu, H. Jiang, W. Zhou, S. Liu, R. Ruan, Integrating continuous-stirred microwave pyrolysis with ex-situ catalytic upgrading for linear low-density polyethylene conversion: Effects of parameter conditions, J. Anal. Appl. Pyrolysis. (2021) 105213.

[13] S. Orozco, J. Alvarez, G. Lopez, M. Artetxe, J. Bilbao, M. Olazar, Pyrolysis of plastic wastes in a fountain confined conical spouted bed reactor: Determination of stable operating conditions, Energy Convers. Manag. 229 (2021) 113768.

[14] R.K. Singh, B. Ruj, A.K. Sadhukhan, P. Gupta, Impact of fast and slow pyrolysis on the degradation of mixed plastic waste: Product yield analysis and their characterization, J.

Energy Inst. 92 (2019) 1647–1657.

[15] J.M. Arandes, M.J. Azkoiti, I. Torre, M. Olazar, P. Castaño, Effect of HZSM-5 catalyst addition on the cracking of polyolefin pyrolysis waxes under FCC conditions, Chem. Eng. J. 132 (2007) 17–26.

[16] J. Agullo, N. Kumar, D. Berenguer, D. Kubicka, A. Marcilla, A. Gómez, T. Salmi, D.Y. Murzin, Catalytic pyrolysis of low density polyethylene over H-β, HY, H-Mordenite, and H-Ferrierite zeolite catalysts: influence of acidity and structures, Kinet. Catal. 48 (2007) 535–540.

[17] C. Muhammad, J.A. Onwudili, P.T. Williams, Catalytic pyrolysis of waste plastic from electrical and electronic equipment, J. Anal. Appl. Pyrolysis. 113 (2015) 332–339. https://doi.org/10.1016/j.jaap.2015.02.016.

[18] J.A. Onwudili, C. Muhammad, P.T. Williams, Influence of catalyst bed temperature and properties of zeolite catalysts on pyrolysis-catalysis of a simulated mixed plastics sample for the production of upgraded fuels and chemicals, J. Energy Inst. 92 (2019) 1337–1347. https://doi.org/10.1016/j.joei.2018.10.001.

[19] Y. Xue, P. Johnston, X. Bai, Effect of catalyst contact mode and gas atmosphere during catalytic pyrolysis of waste plastics, Energy Convers. Manag. 142 (2017) 441–451.

[20] M. Artetxe, G. Lopez, G. Elordi, M. Amutio, J. Bilbao, M. Olazar, Production of light olefins from polyethylene in a two-step process: pyrolysis in a conical spouted bed and downstream high-temperature thermal cracking, Ind. Eng. Chem. Res. 51 (2012) 13915–13923.

[21] S.R. Kulkarni, A. Gonzalez- Quiroga, M. Nuñez, C. Schuerewegen, P. Perreault, C. Goel, G.J. Heynderickx, K.M. Van Geem, G.B. Marin, An experimental and numerical study of the suppression of jets, counterflow, and backflow in vortex units, AIChE J. 65 (2019) e16614.

[22] M. Artetxe, G. Lopez, M. Amutio, G. Elordi, J. Bilbao, M. Olazar, Light olefins from HDPE cracking in a two-step thermal and catalytic process, Chem. Eng. J. 207 (2012) 27–34.

[23] J.F. Mastral, C. Berrueco, M. Gea, J. Ceamanos, Catalytic degradation of high density polyethylene over nanocrystalline HZSM-5 zeolite, Polym. Degrad. Stab. 91 (2006) 3330–3338.

[24] I. Torre, J.M. Arandes, P. Castano, M. Azkoiti, J. Bilbao, H.I. de Lasa, Catalytic cracking of plastic pyrolysis waxes with vacuum gasoil: effect of HZSM-5 zeolite in the FCC catalyst, Int. J. Chem. React. Eng. 4 (2006).

[25] R.H. Harding, A.W. Peters, J.R.D. Nee, New developments in FCC catalyst technology, Appl. Catal. A Gen. 221 (2001) 389–396. https://doi.org/10.1016/S0926-860X(01)00814-6.

[26] Y. Fujiyama, M.H. Al-Tayyar, C.F. Dean, A. Aitani, H.H. Redhwi, Development of high-severity FCC process: an overview, Stud. Surf. Sci. Catal. 166 (2007) 1–12.

[27] I. Vollmer, M.J.F. Jenks, R.M. González, F. Meirer, B.M. Weckhuysen, Plastic Waste Conversion over a Refinery Waste Catalyst, Angew. Chemie Int. Ed. (2021). https://doi.org/10.1002/anie.202104110.

[28] E. Butler, G. Devlin, K. McDonnell, Waste polyolefins to liquid fuels via pyrolysis: review of commercial state-of-the-art and recent laboratory research, Waste and Biomass Valorization. 2 (2011) 227–255.

[29] K.-H. Lee, N.-S. Noh, D.-H. Shin, Y. Seo, Comparison of plastic types for catalytic degradation of waste plastics into liquid product with spent FCC catalyst, Polym. Degrad. Stab. 78 (2002) 539–544.

[30] T.F. Degnan, G.K. Chitnis, P.H. Schipper, History of ZSM-5 fluid catalytic cracking additive development at Mobil, Microporous Mesoporous Mater. 35–36 (2000) 245–252. https://doi.org/10.1016/S1387-1811(99)00225-5.

[31] N. Rahimi, R. Karimzadeh, Catalytic cracking of hydrocarbons over modified ZSM-5 zeolites to produce light olefins: A review, Appl. Catal. A Gen. 398 (2011) 1–17. https://doi.org/10.1016/j.apcata.2011.03.009.

[32] O. Awayssa, N. Al-Yassir, A. Aitani, S. Al-Khattaf, Modified HZSM-5 as FCC additive for enhancing light olefins yield from catalytic cracking of VGO, Appl. Catal. A Gen. 477 (2014) 172–183. https://doi.org/10.1016/j.apcata.2014.03.021.

[33] M.F. Alotibi, B.A. Alshammari, M.H. Alotaibi, F.M. Alotaibi, S. Alshihri, R.M. Navarro, J.L.G. Fierro, ZSM-5 Zeolite Based Additive in FCC Process: A Review on Modifications for Improving Propylene Production, Catal. Surv. from Asia. 24 (2020) 1–10. https://doi.org/10.1007/s10563-019-09285-1.

[34] T. Blasco, A. Corma, J. Martínez-Triguero, Hydrothermal stabilization of ZSM-5 catalytic-cracking additives by phosphorus addition, J. Catal. 237 (2006) 267–277. https://doi.org/10.1016/j.jcat.2005.11.011.

[35] L. Huang, Q. Li, Enhanced Acidity and Thermal Stability of Mesoporous Materials with Post-treatment with Phosphoric Acid, Chem. Lett. (1999) 829–830.

[36] H.E. Van Der Bij, F. Meirer, S. Kalirai, J. Wang, B.M. Weckhuysen, Hexane cracking over steamed phosphated zeolite H-ZSM-5: Promotional effect on catalyst performance and stability, Chem. - A Eur. J. 20 (2014) 16922–16932. https://doi.org/10.1002/chem.201404924.

[37] G. Caeiro, P. Magnoux, J.M. Lopes, F.R. Ribeiro, S.M.C. Menezes, A.F. Costa, H.S. Cerqueira, Stabilization effect of phosphorus on steamed H-MFI zeolites, Appl. Catal. A Gen. 314 (2006) 160–171. https://doi.org/10.1016/j.apcata.2006.08.016.

[38] A. Corma, J. Mengual, P.J. Miguel, Stabilization of ZSM-5 zeolite catalysts for steam catalytic cracking of naphtha for production of propene and ethene, "Applied Catal. A, Gen. 421–422 (2012) 121–134. https://doi.org/10.1016/j.apcata.2012.02.008.

[39] O.D. Mante, F.A. Agblevor, S.T. Oyama, R. McClung, The effect of hydrothermal treatment of FCC catalysts and ZSM-5 additives in catalytic conversion of biomass, Appl. Catal. A Gen. 445–446 (2012) 312–320. https://doi.org/10.1016/j.apcata.2012.08.039.

[40] W. Yao, J. Li, Y. Feng, W. Wang, X. Zhang, Q. Chen, S. Komarneni, Y. Wang, Thermally stable phosphorus and nickel modified ZSM-5 zeolites for catalytic co-pyrolysis of biomass and plastics, RSC Adv. 5 (2015) 1–4. https://doi.org/10.1039/C5RA02947C.

[41] H.E. Van Der Bij, B.M. Weckhuysen, Phosphorus promotion and poisoning in zeolite-based

materials: synthesis, characterisation and catalysis, Chem. Soc. Rev. 44 (2015) 7406–7428. https://doi.org/10.1039/C5CS00109A.

[42] H.E. van der Bij, B.M. Weckhuysen, Local silico-aluminophosphate interfaces within phosphated H-ZSM-5 zeolites, Phys. Chem. Chem. Phys. 16 (2014) 9892. https://doi.org/10.1039/c3cp54791d.

[43] H.E. van der Bij, B.M. Weckhuysen, Phosphorus promotion and poisoning in zeolite-based materials: synthesis, characterisation and catalysis, Chem. Soc. Rev. 44 (2015) 7406–7428. https://doi.org/10.1039/C5CS00109A.

[44] N. Miskolczi, L. Bartha, G. Deák, Thermal degradation of polyethylene and polystyrene from the packaging industry over different catalysts into fuel-like feed stocks, Polym. Degrad. Stab. 91 (2006) 517–526. https://doi.org/10.1016/j.polymdegradstab.2005.01.056.

[45] Y.H. Lin, M.H. Yang, Catalytic conversion of commingled polymer waste into chemicals and fuels over spent FCC commercial catalyst in a fluidised-bed reactor, Appl. Catal. B Environ. 69 (2007) 145–153. https://doi.org/10.1016/j.apcatb.2006.07.005.

[46] J. Mertinkat, A. Kirsten, M. Predel, W. Kaminsky, Cracking catalysts used as fluidized bed material in the Hamburg pyrolysis process, J. Anal. Appl. Pyrolysis. 49 (1999) 87–95. https://doi.org/10.1016/S0165-2370(98)00103-X.

[47] S. Ali, A.A. Garforth, D.H. Harris, D.J. Rawlence, Y. Uemichi, Polymer waste recycling over "used" catalysts, Catal. Today. 75 (2002) 247–255. https://doi.org/10.1016/S0920-5861(02)00076-7.

[48] A. Eschenbacher, P.A. Jensen, U.B. Henriksen, J. Ahrenfeldt, C. Li, J.Ø. Duus, U.V. Mentzel, A.D. Jensen, Impact of ZSM-5 deactivation on bio-oil quality during upgrading of straw derived pyrolysis vapors, Energy & Fuels. 33 (2019) 397–412. https://doi.org/10.1021/acs.energyfuels.8b03691.

[49] A. Eschenbacher, A. Saraeian, B.H. Shanks, U.V. Mentzel, J. Ahrenfeldt, U.B. Henriksen, A.D. Jensen, Counteracting rapid catalyst deactivation by concomitant temperature increase during catalytic upgrading of biomass pyrolysis vapors using solid acid catalysts, Catalysts. (2020). https://doi.org/https://doi.org/10.3390/catal10070748.

[50] M. Ibáñez, M. Artetxe, G. Lopez, G. Elordi, J. Bilbao, M. Olazar, P. Castaño, Identification of the coke deposited on an HZSM-5 zeolite catalyst during the sequenced pyrolysis-cracking of HDPE, Appl. Catal. B Environ. 148–149 (2014) 436–445. https://doi.org/10.1016/j.apcatb.2013.11.023.

[51] C. Engtrakula, C. Mukarakate, A.K. Starace, K. Magrini, A.K. Rogersb, M.M. Yung, C. Engtrakul, A.K. Rogers, T.R. Carlson, G.A. Tompsett, W.C. Conner, G.W. Huber, Effect of ZSM-5 acidity on aromatic product selectivity during upgrading of pine pyrolysis vapors, Catal. Today. 5 (2015) 175–181. https://doi.org/10.1016/j.cattod.2015.10.032.

[52] M. Olazar, G. Lopez, M. Amutio, G. Elordi, R. Aguado, J. Bilbao, Influence of FCC catalyst steaming on HDPE pyrolysis product distribution, J. Anal. Appl. Pyrolysis. 85 (2009) 359–365. https://doi.org/10.1016/j.jaap.2008.10.016.

[53] D.P. Serrano, J. Aguado, J.M. Escola, Developing advanced catalysts for the conversion of polyolefinic waste plastics into fuels and chemicals, ACS Catal. 2 (2012) 1924–1941.

https://doi.org/10.1021/cs3003403.

[54] K.G. Kalogiannis, S.D. Stefanidis, A.A. Lappas, Catalyst deactivation, ash accumulation and bio-oil deoxygenation during ex situ catalytic fast pyrolysis of biomass in a cascade thermal-catalytic reactor system, Fuel Process. Technol. 186 (2019) 99–109. https://doi.org/10.1016/j.fuproc.2018.12.008.

[55] A. Eschenbacher, A. Saraeian, B.H. Shanks, P.A. Jensen, U.B. Henriksen, J. Ahrenfeldt, A.D. Jensen, Insights into the scalability of catalytic upgrading of biomass pyrolysis vapors using micro and bench-scale reactors, Sustain. Energy Fuels. (2020) 22–24. https://doi.org/10.1039/d0se00303d.

[56] A. Eschenbacher, P.A. Jensen, U.B. Henriksen, J. Ahrenfeldt, S. Ndoni, C. Li, J.Ø. Duus, U.V. Mentzel, A.D. Jensen, Catalytic deoxygenation of vapors obtained from ablative fast pyrolysis of wheat straw using mesoporous HZSM-5, Fuel Process. Technol. 194 (2019) 106119. https://doi.org/10.1016/J.FUPROC.2019.106119.

[57] D.S. Achilias, C. Roupakias, P. Megalokonomos, A.A. Lappas, V. Antonakou, Chemical recycling of plastic wastes made from polyethylene (LDPE and HDPE) and polypropylene (PP), J. Hazard. Mater. 149 (2007) 536–542. https://doi.org/10.1016/j.jhazmat.2007.06.076.

[58] J. Aguado, D.P. Serrano, G. San Miguel, M.C. Castro, S. Madrid, Feedstock recycling of polyethylene in a two-step thermo-catalytic reaction system, J. Anal. Appl. Pyrolysis. 79 (2007) 415–423. https://doi.org/10.1016/j.jaap.2006.11.008.

[59] R. Bagri, P.T. Williams, Catalytic pyrolysis of polyethylene, J. Anal. Appl. Pyrolysis. 63 (2002) 29–41. https://doi.org/10.1016/S0165-2370(01)00139-5.

[60] M. Artetxe, G. Lopez, M. Amutio, G. Elordi, J. Bilbao, M. Olazar, Cracking of high density polyethylene pyrolysis waxes on HZSM-5 catalysts of different acidity, Ind. Eng. Chem. Res. 52 (2013) 10637–10645. https://doi.org/10.1021/ie4014869.

[61] S. Chaianansutcharit, R. Katsutath, A. Chaisuwan, T. Bhaskar, A. Nigo, A. Muto, Y. Sakata, Catalytic degradation of polyolefins over hexagonal mesoporous silica: Effect of aluminum addition, J. Anal. Appl. Pyrolysis. 80 (2007) 360–368. https://doi.org/10.1016/j.jaap.2007.04.009.

[62] A. Eschenbacher, P.A. Jensen, U.B. Henriksen, J. Ahrenfeldt, C. Li, J.Ø. Duus, U.V. Mentzel, A.D. Jensen, Deoxygenation of wheat straw fast pyrolysis vapors using HZSM-5, Al2O3 , HZSM-5/Al2O3 extrudates, and desilicated HZSM-5/Al2O3 extrudates, Energy & Fuels. 33 (2019) 6405−6420. https://doi.org/10.1021/acs.energyfuels.9b00906.

[63] G. De La Puente, C. Klocker, U. Sedran, Conversion of waste plastics into fuels recycling polyethylene in FCC, Appl. Catal. B Environ. 36 (2002) 279–285. https://doi.org/10.1016/S0926-3373(01)00287-9.

[64] Y.H. Lin, M.H. Yang, Catalytic pyrolysis of polyolefin waste into valuable hydrocarbons over reused catalyst from refinery FCC units, Appl. Catal. A Gen. 328 (2007) 132–139. https://doi.org/10.1016/j.apcata.2007.05.039.

[65] M.H. Yang, Y.H. Lin, Catalytic Conversion of Postconsumer PE/PP Waste into Hydrocarbons Using the FCC Process with an Equilibrium FCC Commercial Catalyst, J. Appl. Polym. Sci. 114 (2009) 193–203. https://doi.org/10.1002/app.

[66] G. Elordi, M. Olazar, P. Castaño, M. Artetxe, J. Bilbao, Polyethylene cracking on a spent FCC catalyst in a conical spouted bed, Ind. Eng. Chem. Res. 51 (2012) 14008–14017. https://doi.org/10.1021/ie3018274.

[67] P.A. Johnston, Thermochemical methylation of lignin to produce high value aromatic compounds, Iowa State University, 2017. https://lib.dr.iastate.edu/etd/15544.

[68] J.G. Yao, Investigations of the Combination of Carbon Capture and Storage via the Calcium Looping Cycle with Biomass Combustion, (2016).

[69] Y. Nishiyama, S. Kumagai, T. Kameda, Y. Saito, A. Watanabe, C. Watanabe, N. Teramae, T. Yoshioka, Direct Gas-Phase Derivatization by Employing Tandem μ-Reactor-Gas Chromatography/Mass Spectrometry: Case Study of Trifluoroacetylation of 4,4′-Methylenedianiline, Anal. Chem. 92 (2020) 14924–14929. https://doi.org/10.1021/acs.analchem.0c01830.

[70] K. Schofield, The enigmatic mechanism of the flame ionization detector: Its overlooked implications for fossil fuel combustion modeling, Prog. Energy Combust. Sci. 34 (2008) 330–350. https://doi.org/10.1016/j.pecs.2007.08.001.

[71] H. Shafaghat, H.W. Lee, L. Yang, D. Oh, S.C. Jung, G.H. Rhee, J. Jae, Y.K. Park, Catalytic co-conversion of Kraft lignin and linear low-density polyethylene over mesoZSM-5 and Al-SBA-15 catalysts, Catal. Today. (2019) 0–1. https://doi.org/10.1016/j.cattod.2019.04.052.

[72] J. Scheirs, Overview of Commercial Pyrolysis Processes for Waste Plastics, 2006. https://doi.org/10.1002/0470021543.ch15.

[73] S. Hafeez, E. Pallari, G. Manos, A. Constantinou, Catalytic conversion and chemical recovery, Elsevier Inc., 2018. https://doi.org/10.1016/B978-0-12-813140-4.00006-6.

[74] L.H. Ong, M. Dömök, R. Olindo, A.C. Van Veen, J.A. Lercher, Dealumination of HZSM-5 via steam-treatment, Microporous Mesoporous Mater. 164 (2012) 9–20. https://doi.org/10.1016/j.micromeso.2012.07.033.

[75] J.N. Louwen, S. Simko, K. Stanciakova, R.E. Bulo, B.M. Weckhuysen, E.T.C. Vogt, Role of Rare Earth Ions in the Prevention of Dealumination of Zeolite Y for Fluid Cracking Catalysts, J. Phys. Chem. C. 124 (2020) 4626–4636. https://doi.org/10.1021/ACS.JPCC.9B11956.

[76] H.E. van der B. Geboren, Phosphatation of Zeolites : A Combined Spectroscopy , Microscopy and Catalysis Study, 2014.

[77] L. Ballice, R. Reimert, Classification of volatile products from the temperature-programmed pyrolysis of polypropylene (PP), atactic-polypropylene (APP) and thermogravimetrically derived kinetics of pyrolysis, Chem. Eng. Process. 41 (2002) 289–296. https://doi.org/10.1016/S0255-2701(01)00144-1.

[78] M.T.S.P. De Amorim, C. Comel, P. Vermande, Pyrolysis of polypropylene, J. Anal. Appl. Pyrolysis. 4 (1982) 73–81. https://doi.org/10.1016/0165-2370(82)80028-4.

[79] P. Kusch, Application of Pyrolysis-Gas Chromatography/Mass Spectrometry (Py-GC/MS), Elsevier Ltd, 2017. https://doi.org/10.1016/bs.coac.2016.10.003.

[80] I. Çit, A. Sinağ, T. Yumak, S. Uçar, Z. Misirlioğlu, M. Canel, Comparative pyrolysis of

polyolefins (PP and LDPE)and PET, Polym. Bull. 64 (2010) 817–834. https://doi.org/10.1007/s00289-009-0225-x.

[81] S. Qian, H. Ji, X.X. Wu, N. Li, Y. Yang, J. Bu, X. Zhang, L. Qiao, H. Yu, N. Xu, C. Zhang, Detection and quantification analysis of chemical migrants in plastic food contact products, PLoS One. 13 (2018) 1–11. https://doi.org/10.1371/journal.pone.0208467.

[82] M. Arabiourrutia, G. Elordi, G. Lopez, E. Borsella, J. Bilbao, M. Olazar, Characterization of the waxes obtained by the pyrolysis of polyolefin plastics in a conical spouted bed reactor, J. Anal. Appl. Pyrolysis. 94 (2012) 230–237. https://doi.org/10.1016/j.jaap.2011.12.012.

[83] J.L. Agudelo, E.J.M. Hensen, S.A. Giraldo, L.J. Hoyos, Influence of steam-calcination and acid leaching treatment on the VGO hydrocracking performance of faujasite zeolite, Fuel Process. Technol. 133 (2015) 89–96. https://doi.org/10.1016/j.fuproc.2015.01.011.

[84] W. Lutz, C.H. Rüscher, T.M. Gesing, M. Stöcker, S. Vasenkov, D. Freude, R. Gläser, C. Berger, Investigations of the mechanism of dealumination of zeolite Y by steam: Tuned mesopore formation versus the Si/Al ratio, Stud. Surf. Sci. Catal. 154 B (2004) 1411–1417. https://doi.org/10.1016/s0167-2991(04)80658-x.

[85] M. Bjørgen, S. Svelle, F. Joensen, J. Nerlov, S. Kolboe, F. Bonino, L. Palumbo, S. Bordiga, U. Olsbye, Conversion of methanol to hydrocarbons over zeolite H-ZSM-5: On the origin of the olefinic species, J. Catal. 249 (2007) 195–207. https://doi.org/10.1016/j.jcat.2007.04.006.

[86] M. Bjørgen, F. Joensen, K.P. Lillerud, U. Olsbye, S. Svelle, The mechanisms of ethene and propene formation from methanol over high silica H-ZSM-5 and H-beta, Catal. Today. 142 (2009) 90–97. https://doi.org/10.1016/j.cattod.2009.01.015.

[87] U. Olsbye, S. Svelle, M. Bjrgen, P. Beato, T.V.W. Janssens, F. Joensen, S. Bordiga, K.P. Lillerud, Conversion of methanol to hydrocarbons: How zeolite cavity and pore size controls product selectivity, Angew. Chemie - Int. Ed. 51 (2012) 5810–5831. https://doi.org/10.1002/anie.201103657.

[88] M. Artetxe, G. Lopez, M. Amutio, J. Bilbao, M. Olazar, Kinetic modelling of the cracking of HDPE pyrolysis volatiles on a HZSM-5 zeolite based catalyst, Chem. Eng. Sci. 116 (2014) 635–644. https://doi.org/10.1016/j.ces.2014.05.044.

[89] K.B. Park, Y.S. Jeong, B. Guzelciftci, J.S. Kim, Characteristics of a new type continuous two-stage pyrolysis of waste polyethylene, Energy. 166 (2019) 343–351. https://doi.org/10.1016/j.energy.2018.10.078.

[90] K.B. Park, Y.S. Jeong, J.S. Kim, Activator-assisted pyrolysis of polypropylene, Appl. Energy. 253 (2019) 113558. https://doi.org/10.1016/j.apenergy.2019.113558.

[91] A. Akah, M. Al-Ghrami, Maximizing propylene production via FCC technology, Appl. Petrochemical Res. 5 (2015) 377–392. https://doi.org/10.1007/s13203-015-0104-3.

[92] X. Meng, C. Xu, J. Gao, L. Li, Studies on catalytic pyrolysis of heavy oils: Reaction behaviors and mechanistic pathways, Appl. Catal. A Gen. 294 (2005) 168–176. https://doi.org/10.1016/j.apcata.2005.07.033.

[93] A.I. Hussain, A.M. Aitani, M. Kubů, Jиc. Čejka, S. Al-Khattaf, Catalytic cracking of Arabian Light VGO over novel zeolites as FCC catalyst additives for maximizing propylene yield,

Fuel. 167 (2016) 226–239. https://doi.org/10.1016/j.fuel.2015.11.065.

[94] P.P. Plehiers, S.H. Symoens, I. Amghizar, G.B. Marin, C. V. Stevens, K.M. Van Geem, Artificial Intelligence in Steam Cracking Modeling: A Deep Learning Algorithm for Detailed Effluent Prediction, Engineering. 5 (2019) 1027–1040. https://doi.org/10.1016/j.eng.2019.02.013.

[95] J.-P. Lange, Towards circular carbo-chemicals – the metamorphosis of petrochemicals, Energy Environ. Sci. (2021). https://doi.org/DOI: 10.1039/D1EE00532D.